

CONFIDENTIAL

Copy
RM L53D29a

NACA RM L53D29a

NACA

RESEARCH MEMORANDUM

LOADS DUE TO FLAPS AND SPOILERS ON SWEEPBACK WINGS
AT SUBSONIC AND TRANSONIC SPEEDS

By Alexander D. Hammond and F. E. West, Jr.

Langley Aeronautical Laboratory
Langley Field, Va.

~~CLASSIFICATION CHANGED~~

UNCLASSIFIED

To

By authority

*NACA Rec also effective
RN-126
APR 15 1958*

CLASSIFIED DOCUMENT

This material contains information affecting the National Defense of the United States within the meaning of the espionage laws, Title 18, U.S.C., Secs. 793 and 794, the transmission or revelation of which in any manner to an unauthorized person is prohibited by law.

NATIONAL ADVISORY COMMITTEE FOR AERONAUTICS

WASHINGTON

June 22, 1953

CONFIDENTIAL



NATIONAL ADVISORY COMMITTEE FOR AERONAUTICS

RESEARCH MEMORANDUM

LOADS DUE TO FLAPS AND SPOILERS ON SWEEPBACK WINGS

AT SUBSONIC AND TRANSONIC SPEEDS

By Alexander D. Hammond and F. E. West, Jr.

SUMMARY

A summary is presented of the available data on the loads associated with deflection of controls on thin sweptback wings at high subsonic and transonic speeds. The results show that the centers of pressure of the additional loads resulting from control deflection are in general farther forward for spoiler-type controls than for flap-type controls. The centers of additional load resulting from deflection of flap-type controls may be estimated at subsonic speeds in the low angle-of-attack range by existing theory. The variation of the centers of additional loads resulting from control deflections with angle of attack and Mach numbers through the transonic speed range may be obtained either from pressure distribution data or force-data results from semispan investigations of the controls. Spoiler loads may be estimated if the wing pressures immediately ahead of and behind the spoiler are known.

INTRODUCTION

One of the important considerations in the structural design of wings with controls for high-speed aircraft is the loads resulting from control deflection. In the past, most of the available data that show the effect of flaps (refs. 1 to 5) and spoilers (refs. 6 and 7) on wing loads at high subsonic and transonic speeds have been obtained on moderately thick or very thick wings. This paper presents results of some of the more recent data that show the loads which result from deflection of flaps and spoilers and their point of application on thin sweptback wings at high subsonic and transonic speeds. Also shown are the loads on a spoiler on a typical sweptback-wing configuration.

COEFFICIENTS AND SYMBOLS

$\Delta c_{m_{c/4}}$	incremental section pitching-moment coefficient resulting from control deflection, measured about the local quarter-chord line, $\frac{\text{Incremental pitching moment}}{qc^2}$
Δc_n	incremental section normal-force coefficient resulting from control deflection, $\frac{\text{Incremental normal force}}{qc}$
C_{N_s}	spoiler normal-force coefficient, $\frac{\text{Spoiler normal force}}{qS_s}$
P	pressure coefficient, $\frac{P - P_0}{q}$
P_u	pressure coefficient on wing upper surface
P_l	pressure coefficient on wing lower surface
P_R	resultant pressure coefficient, $P_u - P_l$
ΔP_R	incremental resultant pressure coefficient resulting from control deflection
A	aspect ratio, b^2/S
b	wing span, ft
b_f	control span, ft
c	local wing chord measured in planes parallel to wing plane of symmetry, ft
c_r	root chord of wing, ft
c_t	tip chord of wing, ft
\bar{c}	wing mean aerodynamic chord, $\frac{2}{S} \int_0^{b/2} c^2 dy$, ft

h	spoiler height measured from wing surface, ft
M	Mach number
p	static pressure, lb/sq ft
p_o	free-stream static pressure, lb/sq ft
q	free-stream dynamic pressure, $\frac{1}{2}\rho V^2$, lb/sq ft
S	wing area, sq ft
S_s	spoiler area, sq ft
V	free-stream air velocity, ft/sec
x	chordwise distance from wing leading edge, ft
Δx_{cp}	chordwise distance of the center of additional load resulting from control deflection from wing leading edge, ft
y	spanwise distance from plane of symmetry, ft
Δy_{cp}	spanwise distance of the center of additional load resulting from control deflection from plane of symmetry, ft
y_{cps}	spanwise distance of the center of pressure of the spoiler load from the plane of symmetry, ft
z	vertical distance from wing surface
α	angle of attack of wing, deg
δ	control deflection
Λ	sweep angle, deg
λ	taper ratio; ratio of tip chord to root chord, c_t/c_r
ρ	mass density of air, slugs/cu ft

DISCUSSION

Figure 1 shows some chordwise pressure-distribution measurements obtained in the Langley high-speed 7- by 10-foot tunnel at the midsemispan

station of a semispan model (refs. 8 and 9). The wing had 35° sweepback of the quarter-chord line, an aspect ratio of 4.0, a taper ratio of 0.6, and an NACA 65A006 airfoil section parallel to the plane of symmetry. The pressure distributions show how the resultant pressure ΔP_R caused by the projection of a plug-type spoiler (that is, a spoiler with a slot through the wing behind the spoiler when the spoiler is deflected) and the deflection of a 20-percent-chord flap is distributed across the wing chord. The results are for a spoiler projection of $0.04c$ and a flap deflection δ of 15° . These distributions are shown for angles of attack α of 0° and 16° at Mach numbers of 0.60 and 0.90. It is evident from the pressure distributions at a Mach number of 0.60 and at 0° angle of attack that the center of pressure is farther forward for the spoiler than for the flap, since the loading on the flap is large, whereas the loading on the wing behind the spoiler is small. As the Mach number is increased from 0.60 to 0.90, the center of pressure of the flap moves rearward as does the center of pressure for the spoiler. At the large angles of attack at either Mach number, the gap behind this deflected spoiler is not sufficient to produce much control effectiveness and there is little change in center-of-pressure location. The center of pressure moves rearward, however, with increase in angle of attack for either positive or negative flap deflection at both Mach numbers.

The longitudinal center of pressure of the additional load resulting from spoiler and flap deflection has also been obtained, for the symmetrical-loading case, from force-data results on semispan wings equipped with these controls. Figure 2 shows the span and spanwise locations of flap and spoiler configurations that were investigated at transonic speeds on a small-scale semispan model in the Langley high-speed 7- by 10-foot tunnel. The model had the quarter chord swept back 45° , an aspect ratio of 4.0, a taper ratio of 0.6, and an NACA 65A006 airfoil section parallel to the plane of symmetry. In the upper half of the figure are shown several span outboard flaps (flaps starting at the wing tip and extending inboard) and one inboard flap (a flap starting at the inboard end of the wing and extending outboard). The flap configurations were tested utilizing the transonic-bump method (ref. 10). In the lower half of the figure are shown several span inboard spoilers that were tested on a small reflection plane (results are as yet unpublished).

The loads resulting from symmetrical control deflection may be obtained directly from semispan investigations. The location of the longitudinal center of pressure measured from the quarter chord of the mean aerodynamic chord \bar{c} and expressed as a fraction of \bar{c} is the ratio of the incremental pitching-moment coefficient to the incremental lift coefficient. The location of the lateral center of pressure measured from the plane of symmetry and expressed as a fraction of the wing semispan is the ratio of the incremental root bending-moment coefficient to the incremental lift coefficient.

Figure 3 shows a typical example at a Mach number of 0.60 of the results that can be obtained from semispan tests and shows the loci of the centers of additional load resulting from deflection of the spoilers and flaps at near 0° angle of attack. The symbols shown below the configurations of figure 2 were plotted on the 45° sweptback-wing plan form at the location of the centers of additional load for the corresponding configurations. These locations of the centers of additional load hold for deflections of the 30-percent-chord flaps through a range of $\pm 20^\circ$. The spoilers located along the 70-percent-chord line were projected 10 percent of the local chord. Although appreciable differences exist in the lateral positions of the centers of additional load resulting from deflection of the various span spoilers and flaps, there is very little effect of control span on the chordwise position of the centers of additional load. The centers of additional load resulting from projection of the various span spoilers fall approximately along the 34-percent-chord line and are farther forward than the centers of additional load resulting from deflection of the various span flaps which fall approximately along the 48-percent-chord line.

Figure 4 shows the variation at low angles of attack of these common chord lines $\frac{\Delta x_{cp}}{c}$ with Mach number for a series of model configurations which differ only in wing sweep from the flap configurations shown in figure 2. Data for the flap configurations having sweep angles of 0° , 35° , and 60° were obtained from the results published in references 11, 12, and 13, respectively. The results shown for the 45° swept wing were obtained from the same investigations as the data presented in figure 3 (ref. 10 and unpublished data). The results show that, as the Mach number is increased, the centers of additional load resulting from deflection of the flaps move rearward and, at the highest Mach number, lie along the 80- to 90-percent-chord lines. There seems to be only a small effect of wing sweep on this movement, except that the rearward movement is delayed to a higher Mach number for the swept wings. The curve for inboard spoilers on the 45° swept wing shows that there is considerably less movement of the longitudinal center of additional load with increase in Mach number than there is for the flaps; in fact, there is a slight forward movement at Mach numbers above 0.90.

Figure 5 shows the variation of the lateral center of additional load $\frac{\Delta y_{cp}}{b/2}$ (which is measured from the plane of symmetry and expressed as a fraction of the wing semispan) with control span for the outboard flaps (that is, flaps starting at the wing tip and extending inboard) on the wings referred to in the discussion of figure 4. The results are shown for Mach numbers of 0.60 and 1.10. At a Mach number of 0.60 the lateral center of additional load resulting from flap deflection moves inboard with increase in flap span. This variation is greater for the swept wings than for the unswept wing. Also, the center of additional

load resulting from flap deflection is farther outboard for the small span controls on the swept wings than on the unswept wing; however, as the Mach number is increased to 1.10, the center of additional load resulting from flap deflection moves inboard with increase in flap span at about the same rate for all the wings. There is, in general, a

nearly linear variation of the lateral center of additional load $\frac{\Delta y_{cp}}{b/2}$ resulting from flap deflection with increase in Mach number between 0.60 and 1.10 for all flap configurations investigated. This variation is illustrated in figure 6 for 43-percent-semispan flap-type controls on the 45° sweptback wing; however, the shift of the lateral center of additional load with increase in Mach number may not be as shown for other span controls on other swept wings, although the variation is nearly linear for the other configurations. The curve for the inboard 43-percent-semispan spoilers also shows a nearly linear variation of the lateral center of additional load with increase in Mach number and, in general, shows the same trend as the inboard flap-type controls on the 45° swept wing.

In figure 7 is shown the theoretical and experimental variation of the lateral center of additional load $\frac{\Delta y_{cp}}{b/2}$ resulting from control deflection with control span at a Mach number of 0.60 on the 45° swept-wing configurations of figure 2. The theoretical variation of the lateral center of additional load is shown for symmetrically deflected outboard and inboard flaps. This variation was obtained from theoretical control loadings by an adaptation of the method outlined in reference 14 by assuming an increase in angle of attack of 1 radian over the flapped portion of the wing semispan. The loading and lateral center of pressure may be obtained by integrating the loading curve over the semispan. The symbols represent the experimental points for the control configurations of figure 2. There is good agreement between the experimental and theoretical values for the flap-type controls. Similar agreement can be obtained for flap-type controls on wings of other sweeps and, hence, in the low angle-of-attack range, the variation of the lateral center of load resulting from flap deflection with control span can be estimated for Mach numbers up to at least 0.60.

As the span of the inboard spoilers is increased, the lateral center of load moves outboard and, in general, is slightly outboard of the theoretical curve for the flap for most spoiler spans. This fact indicates that, although the magnitude of the lateral center of additional load may not be predicted from the flap theory, the trend of the variation of the center of additional load with span for inboard spoilers is similar to the trend shown for inboard flaps.

Thus far, the centers of additional load at small angles of attack have been discussed. Figure 8 shows the variation of the longitudinal

$\frac{\Delta x_{cp}}{c}$ and lateral $\frac{\Delta y_{cp}}{b/2}$ locations of the centers of additional load resulting from spoiler projection on a 45° swept wing with angle of attack for Mach numbers of 0.60 and 0.98. The longitudinal positions of the center of additional load $\frac{\Delta x_{cp}}{c}$ were measured from the wing leading edge and are expressed as a fraction of the local wing chord c at the lateral positions of the center of additional load $\frac{\Delta y_{cp}}{b/2}$. The values of $\frac{\Delta y_{cp}}{b/2}$ were measured from the fuselage center line and expressed as fractions of the wing semispan $b/2$. These data were recently obtained from integrated pressure distributions at seven spanwise stations on a sting-supported model in the Langley 16-foot transonic tunnel.

The 45° swept wing is similar to that shown in figure 2; however, the Reynolds number based on the wing mean aerodynamic chord was about 6×10^6 at a Mach number of 1.0 for this model and only about 0.75×10^6 at this Mach number for the model of figure 2. The spoiler was of the plug type and was projected to a height of 4 percent of the local wing chord. It was located along the 70-percent-chord line and extended from the wing-fuselage junction ($0.14b/2$) to the 87-percent-semispan station.

The variation of the longitudinal centers of additional load $\frac{\Delta x_{cp}}{c}$ shows a rather irregular behavior with angle of attack at Mach numbers of 0.60 and 0.98. The lateral centers of additional load show an inboard movement above angles of attack of approximately 10° for both Mach numbers; this inboard movement indicates that the largest changes in the bending moments will occur in the low angle-of-attack range. The irregular trends of the longitudinal centers of additional load and the inboard movement of the lateral centers of additional load are caused by flow separation over the outboard wing sections at the higher angles of attack.

The weighted spanwise loading parameters at a Mach number of 0.98 associated with the centers of additional load in figure 8 are shown in figure 9. The variations of the weighted section normal force $\Delta c_{n_c}/\bar{c}$ and the weighted section pitching moment $\Delta c_{m_c}/4(c/\bar{c})^2$ across the semispan are shown for several angles of attack. The vertical dashed line shown in figure 9 represents the spanwise location of the fuselage maximum diameter. Irregular trends of the section pitching-moment parameter with angle of attack are shown here with increase in angle of attack. Also shown is a loss in effectiveness of the control on the outboard sections of the wing at 16° angle of attack which results from flow separation over the outboard wing sections. This loss of effectiveness causes the inboard shift in the lateral center of additional load

and results in small incremental section pitching moments over the out-board wing sections. The results shown are for one spoiler configuration on a 45° swept wing and may not be typical of the variation of the load distributions on other plan forms. For example, had leading-edge devices designed to improve the flow over the wing been employed in conjunction with the spoiler on this wing, or had the spoiler configuration been improved so as to increase the effectiveness of the control over the separated-flow region of the wing, the trends of the variation of the centers of additional load and of the span loadings with angle of attack would not be expected to be as shown. The load distributions and centers of additional load vary considerably; this variation depends on both the spoiler effectiveness and on the flow-separation phenomenon associated with the wing plan form.

Loadings for the plug-type spoiler, which is described in the discussion of figures 8 and 9, are presented in figure 10. This figure shows how the pressure coefficients P are distributed over the front and rear faces of the plug-type spoiler (shown by the dashed curve) at three spanwise stations for a Mach number of 0.98 and angles of attack of 0° and 16° . The solid curve shows the distributions over the front and rear faces of the same spoiler without a gap through the wing. These pressure distributions were measured over the front and rear faces of the spoiler by using pressure orifices distributed from the wing surface to the top of the spoiler at several spanwise stations. The pressure distributions shown are typical of those obtained at other angles of attack and Mach numbers and show that both with and without a gap through the wing behind the spoiler the loading is generally rectangular and the pressure coefficients are generally more positive over the front face of the spoiler than the rear face. The results also show that the loading is generally less for the plug-type spoiler than for the spoiler without a gap. Figure 11 shows for the spoiler without a gap how the resultant spoiler normal-force coefficient C_{N_B} varies with angle of attack at Mach numbers of 0.60 and 0.98 and how the spoiler lateral center of pressure $\frac{y_{cp_B}}{b/2}$ varies with angle of attack at a Mach number of 0.98. The solid curves of figure 11 were obtained by integrating pressure distributions similar to those shown in figure 10. Also shown as a dashed line connecting the circle symbols are the estimated values of the spoiler normal force and lateral center of pressure obtained by assuming the spoiler sectional loading is rectangular and equal to the difference between the wing pressures measured immediately ahead of and behind the spoiler. These curves show fair agreement with the measured values and show that the spoiler loads may be estimated if the wing pressures ahead of and behind the spoiler are known.

The results show that there is a decrease in spoiler normal-force coefficient and an inboard movement of the lateral center of pressure with increase in angle of attack as is indicated by the pressure distributions of figure 10 for the outboard stations at 16° angle of attack.

CONCLUSIONS

The results show that the centers of pressure of the additional loads resulting from control deflection are, in general, farther forward for spoiler-type controls than for flap-type controls. The centers of additional load resulting from deflection of flap-type controls may be estimated at subsonic speeds in the low angle-of-attack range by existing theory. The variation of the centers of additional loads resulting from control deflections with angle of attack and Mach number through the transonic speed range may be obtained either from pressure distributions or force-data results from semispan investigations of the controls. Spoiler loads may be estimated if the wing pressures immediately ahead of and behind the spoiler controls are known.

Langley Aeronautical Laboratory,
National Advisory Committee for Aeronautics,
Langley Field, Va.

REFERENCES

1. Luoma, Arvo A.: An Investigation of a High-Aspect-Ratio Wing Having 0.20-Chord Plain Ailerons in the Langley 8-Foot High-Speed Tunnel. NACA RM L6H28d, 1946.
2. Luoma, Arvo A., Bielat, Ralph P., and Whitcomb, Richard T.: High-Speed Wind-Tunnel Investigation of the Lateral-Control Characteristics of Plain Ailerons on a Wing With Various Amounts of Sweep. NACA RM L7I15, 1947.
3. Whitcomb, Richard T.: A Compilation of the Pressures Measured on a Wing and Aileron With Various Amounts of Sweep in the Langley 8-Foot High-Speed Tunnel. NACA RM L8A30a, 1948.
4. Krumm, Walter J.: Pressure Coefficients at Mach Numbers From 0.60 to 0.85 for a Semispan Wing With NACA 0012-64 Section, 20-Percent-Chord Plain Aileron, and 0° and 45° Sweepback. NACA RM A50B13, 1950.
5. Krumm, Walter J., and Cleary, Joseph W.: High-Speed Aerodynamic Characteristics of a Lateral-Control Model. III - Section Characteristics, Fence Studies, and Tabulated Pressure Coefficients With Modified NACA 0012-64 Section, 26.6-Percent-Chord, Plain Aileron, 0° and 45° Sweepback. NACA RM A50H17, 1950.
6. Laitone, Edmund V.: An Investigation of the High-Speed Lateral-Control Characteristics of a Spoiler. NACA ACR 4C23, 1944.
7. Luoma, Arvo A.: An Investigation of the Lateral-Control Characteristics of Spoilers on a High-Aspect-Ratio Wing of NACA 65-210 Section in the Langley 8-Foot High-Speed Tunnel. NACA RM L7D21, 1947.
8. Hammond, Alexander D., and McMullan, Barbara M.: Chordwise Pressure Distribution at High Subsonic Speeds Near Midsemispan of a Tapered 35° Sweptback Wing of Aspect Ratio 4 Having NACA 65A006 Airfoil Sections and Equipped With Various Spoiler Ailerons. NACA RM L52C28, 1952.
9. Hammond, Alexander D., and Keffer, Barbara M.: The Effect at High Subsonic Speeds of a Flap-Type Aileron on the Chordwise Pressure Distribution Near Midsemispan of a Tapered 35° Sweptback Wing of Aspect Ratio 4 Having NACA 65A006 Airfoil Section. NACA RM L53C23, 1953.

10. Vogler, Raymond D.: Lateral-Control Investigation of Flap-Type Controls on a Wing With Quarter-Chord Line Swept Back 45° , Aspect Ratio 4, Taper Ratio 0.6, and NACA 65A006 Airfoil Section. Transonic-Bump Method. NACA RM L9F29a, 1949.
11. Hammond, Alexander D.: Lateral-Control Investigation of Flap-Type Controls on a Wing With Unswept Quarter-Chord Line, Aspect Ratio 4, Taper Ratio 0.6, and NACA 65A006 Airfoil Section. Transonic-Bump Method. NACA RM L50A03, 1950.
12. Thompson, Robert F.: Lateral-Control Investigation of Flap-Type Controls on a Wing With Quarter-Chord Line Swept Back 35° , Aspect Ratio 4, Taper Ratio 0.6, and NACA 65A006 Airfoil Section. Transonic-Bump Method. NACA RM L9L12a, 1950.
13. Vogler, Raymond D.: Lateral-Control Investigation of Flap-Type Controls on a Wing With Quarter-Chord Line Swept Back 60° , Aspect Ratio 4, Taper Ratio 0.6, and NACA 65A006 Airfoil Section. Transonic-Bump Method. NACA RM L50A17, 1950.
14. Campbell, George S.: A Finite-Step Method for the Calculation of Span Loadings of Unusual Plan Forms. NACA RM L50L13, 1951.

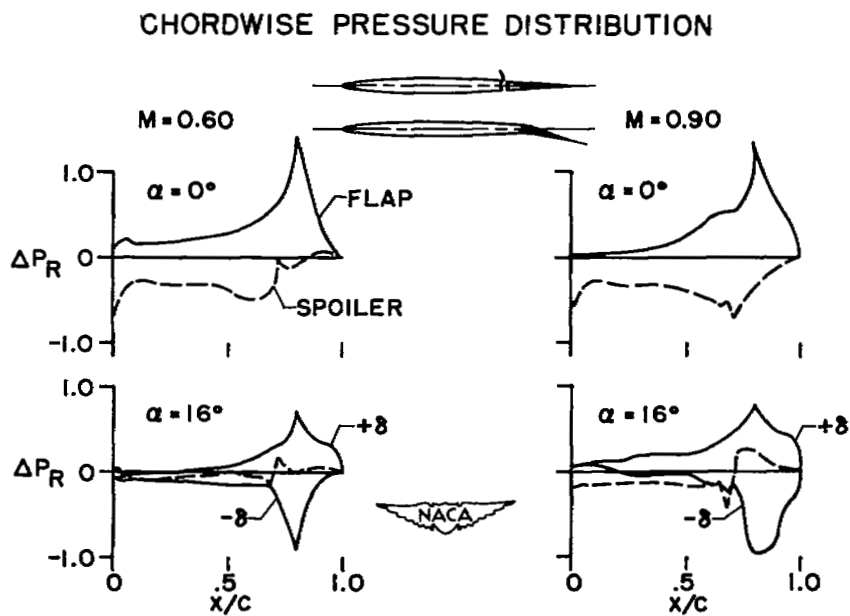


Figure 1.

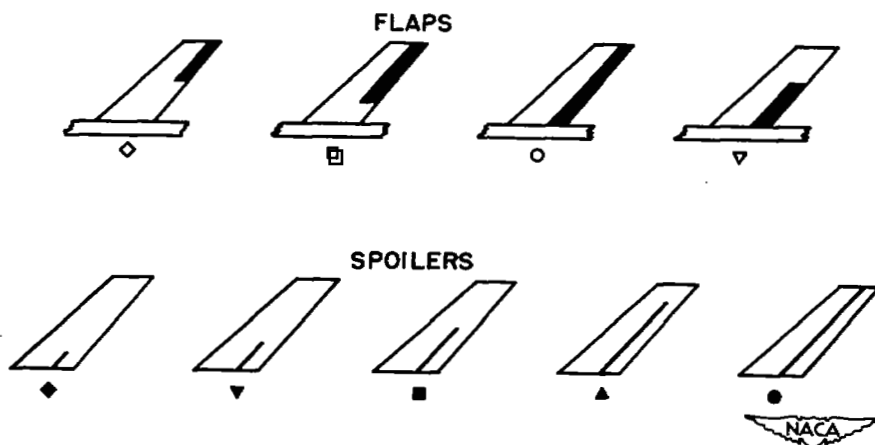
CONTROL CONFIGURATIONS**45° SWEEPED WING**

Figure 2.

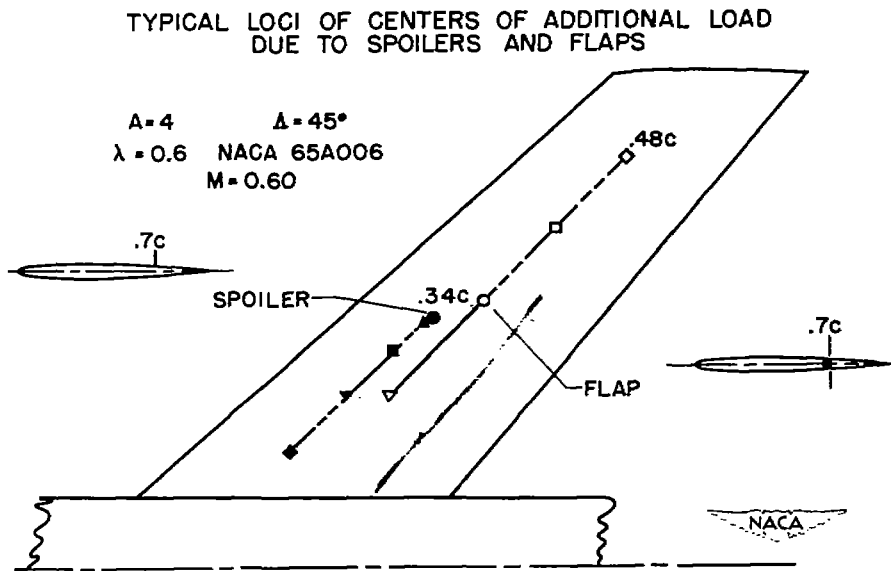


Figure 3.

CHORDWISE CENTERS OF ADDITIONAL LOAD DUE TO
SPOILERS AND FLAPS

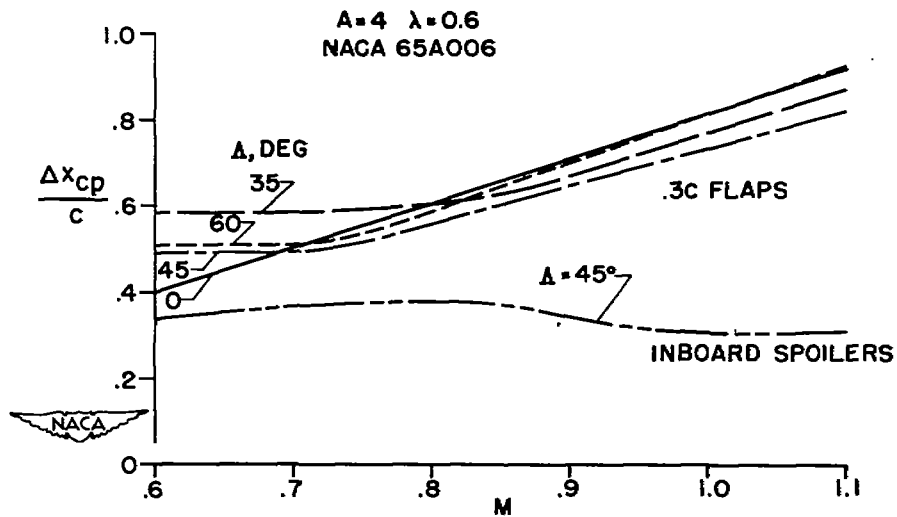


Figure 4.

LATERAL CENTERS OF ADDITIONAL LOAD
DUE TO OUTBOARD FLAPS

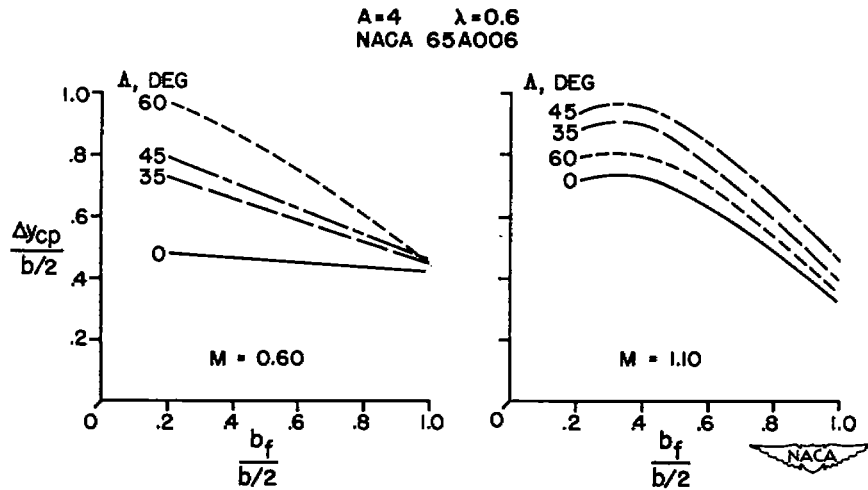


Figure 5.

LATERAL CENTER OF ADDITIONAL LOAD
EFFECT OF MACH NUMBER

A=4; $\Delta=45^\circ$; CONTROL SPAN, $0.43 b/2$

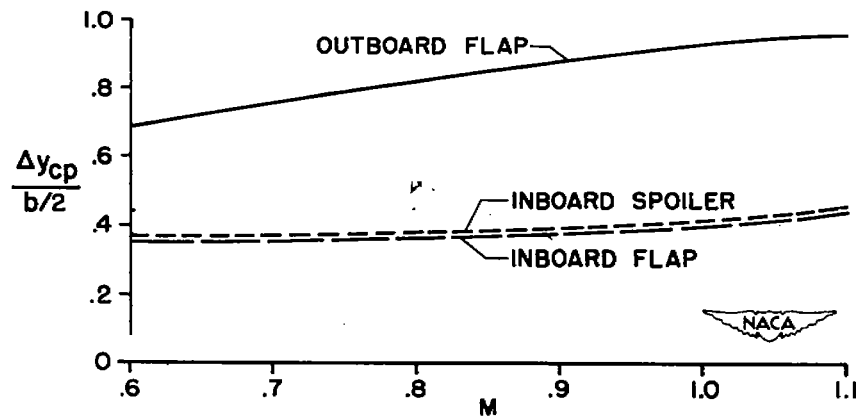


Figure 6.

LATERAL CENTER OF ADDITIONAL LOAD
EFFECT OF CONTROL SPAN

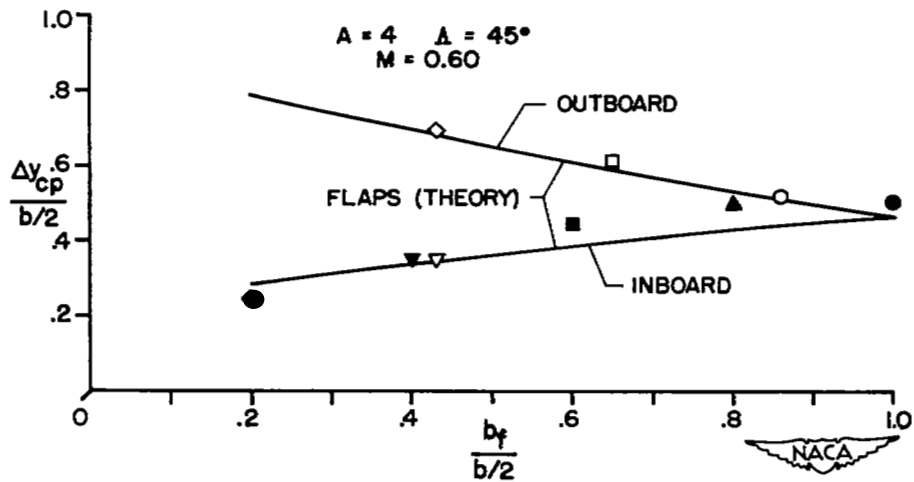


Figure 7.

CENTER OF ADDITIONAL LOAD
DUE TO SPOILER

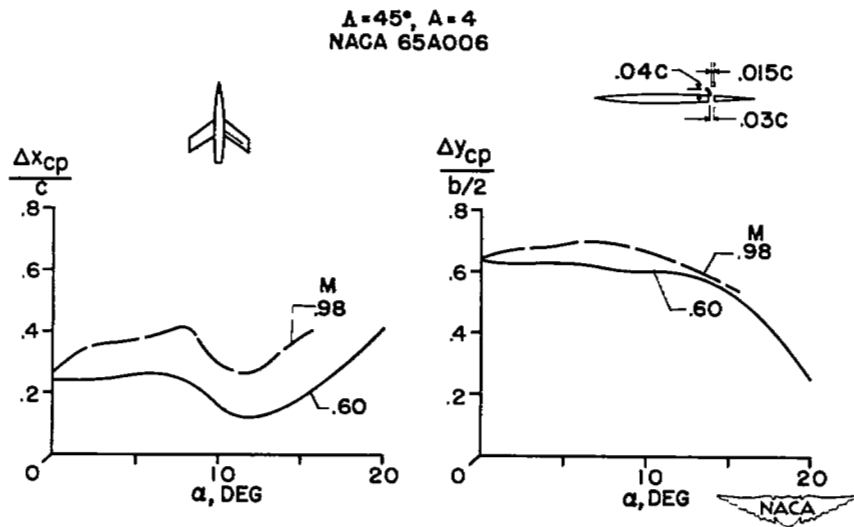


Figure 8.

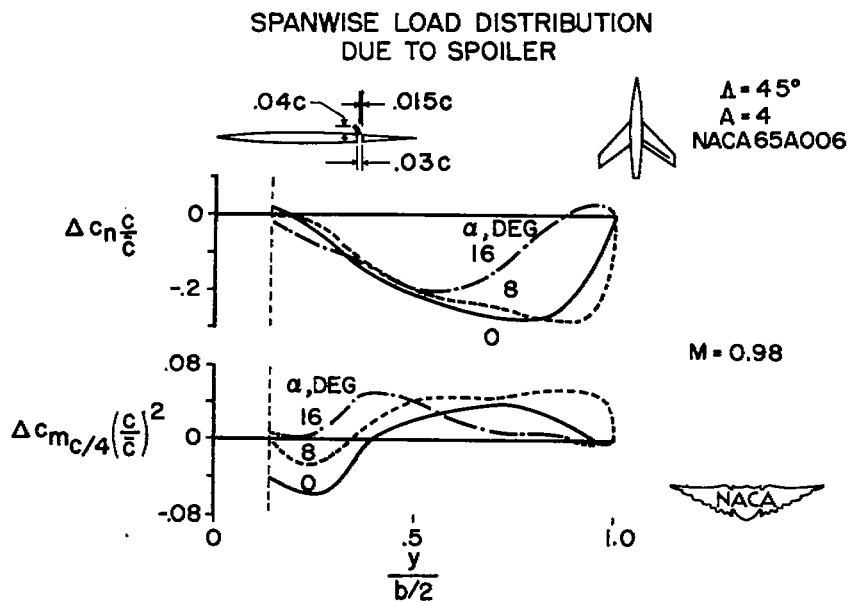


Figure 9.

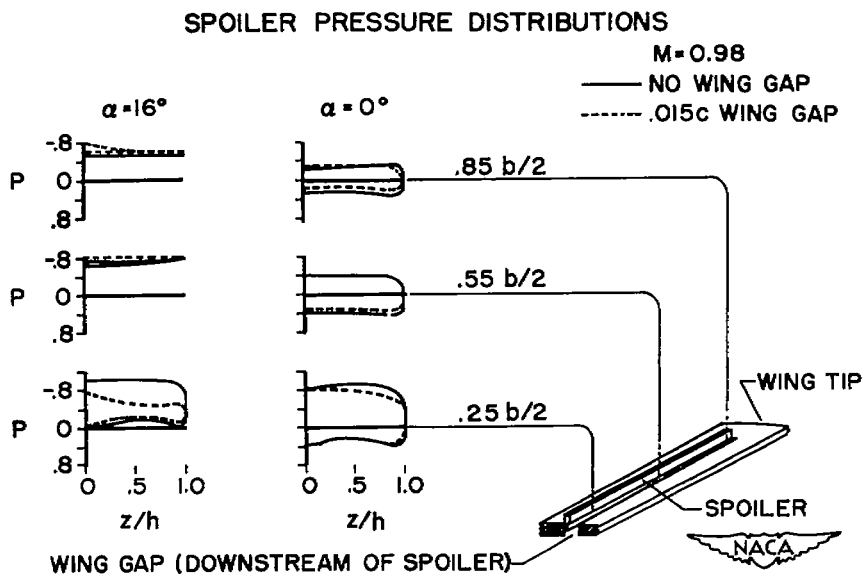


Figure 10.

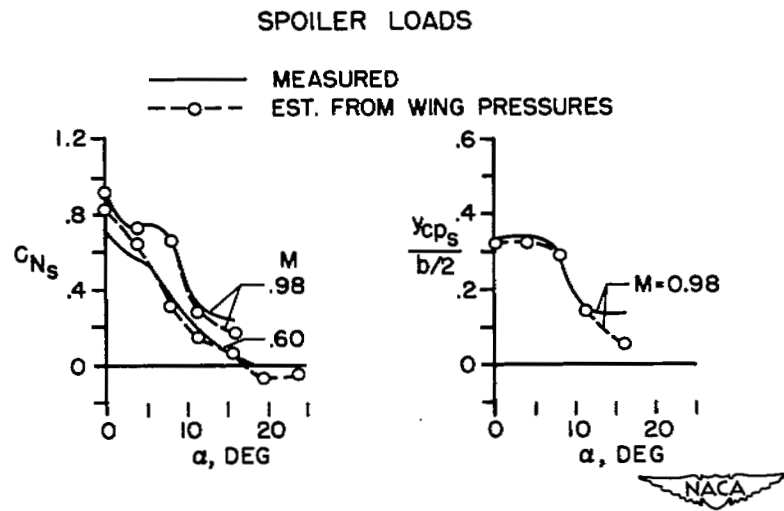


Figure 11.

NASA Technical Library



3 1176 01436 9921

